Environmental Modelling and Software 176 (2024) 106032

Contents lists available at ScienceDirect

Environmental Modelling and Software

journal homepage: www.elsevier.com/locate/envsoft

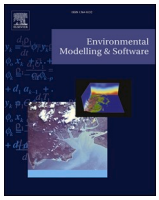

A source apportionment and air quality planning methodology for NO_2 pollution from traffic and other sources

Bart Degraeuwe [a,*], Hans Hooyberghs [a], Stijn Janssen [a], Wouter Lefebvre [a], Bino Maiheu [a,1], Athanasios Megaritis [b], Marlies Vanhulsel [a]

[a] Flemish Institute for Technological Research (VITO), Boeretang 200, 2600, Mol, Belgium
[b] Concawe, Boulevard du Souverain 165, 1160, Brussels, Belgium

ARTICLE INFO

Handling Editor: Daniel P Ames

Keywords:
NO_2
Source-apportionment
Traffic
SHERPA
QUARK

ABSTRACT

In view of upcoming more stringent air quality limits and the ambition to align with the WHO guidelines, nitrogen dioxide (NO_2) pollution from traffic and other sources will remain a problem in the EU. To assess the impact of traffic measures and emission reductions in other sectors on NO_2-concentrations, an EU-wide high-resolution NO_2 source apportionment web-application was developed. The application allows users to define scenarios in a user-friendly way and quickly visualize the NO_2-concentrations at measurement stations and in cities. The user can configure a new Euro 7/VII emission standard and additionally define urban access regulations scenarios in cities. To capture the spatial scales of NO_2 pollution, the SHERPA source-receptor model was used in combination with the QUARK kernel dispersion model. The first model considers long-distance impacts, the latter considers the strong concentration gradients close to roads. This paper focuses on the methodology, a follow-up paper describes the web-application.

Software and data availability section

Software name: NO2 source apportionment.
Developer: VITO N.V.
First year available: 2023.
Hardware requirements: PC.
Software requirements: R statistical environment and language. Additional libraries plyr and yaml.
Program language: R.
Program size: 85.8 MB.
Availability: https://github.com/VITObelgium/NO2_source_apportionment.

The necessary data to run the program are available in the repository under the data folder.

1. Introduction

In this paper we present a methodology to assess the impact of nitrogen oxide (NO_x) emissions on the nitrogen dioxide (NO_2) concentration in cities and at measurement stations. Because road transport is a major source of NO_x emissions, the focus is on international, national, and local measures mitigating these emissions. The impact of both EU-wide regulation (a new emission standard) and local traffic policies (e.g., a low-emission zone) can be studied. Besides road transport, the contribution of other sectors can also be assessed. The methodology allows calculating the effects of a wide range of measures in a matter of seconds. This makes the methodology suitable to be integrated in an interactive web-application. This application allows users that are not familiar with complex air quality models to explore measures to further reduce NO_2 pollution. A second paper will focus on the architecture of the application and present some examples.

On the 22nd of September 2021, the World Health Organisation (WHO) revised its global air quality (AQ) guidelines (World Health Organization, 2021), recommending lower values for most air pollutants that are of concern. For the NO_2 annual average the guideline value was lowered from 40 $\mu g/m^3$ to 10 $\mu g/m^3$. The new guidelines also introduced a 24-h average NO_2 concentration of 25 $\mu g/m^3$ not to be exceeded more than 3–4 times per year. These new guidelines are based on epidemiological studies about the health effects of NO_2 exposure. Specifically, for the EU27 the European Environmental Agency (EEA) estimates that in

* Corresponding author.
E-mail address: bart.degraeuwe@vito.be (B. Degraeuwe).
[1] Currently at the Flemish Environment Agency (VMM).

https://doi.org/10.1016/j.envsoft.2024.106032
Received 7 December 2023; Received in revised form 26 March 2024; Accepted 27 March 2024
Available online 1 April 2024

2020 49,000 premature deaths were attributable to exposure to NO_2 concentrations above the revised WHO guideline level of 10 μg/m^3 (EEA, 2022). As a reaction on the revised WHO AQ guidelines and as part of the European Green Deal's zero-pollution ambition, the European Commission, on the 26th of October 2022, presented its proposal for a revised Ambient Air Quality Directive (AAQD) that includes stricter air quality standards (European Commission, 2022a). The revision proposes as annual average NO_2 limit a value of 20 μg/m^3 instead of the current limit of 40 μg/m^3. As daily average value, not be exceeded more than 18 times per year, 50 μg/m^3 is proposed. The current hourly limit of 200 μg/m^3 should not be exceeded more than once per year instead of 18 times (European Commission, 2022b). According to the proposal, the new EU standards should be met by 2030 and a full alignment with the 2021 WHO AQ guidelines should be achieved by 2050.

Despite that emission reduction measures have significantly reduced NO_2 concentrations in Europe over the last decades, it is likely that additional measures will be necessary to meet the newly proposed EU standards, and even stricter measures to ensure full alignment with the WHO AQ guidelines. At the same time, air quality is a multi-scale and multifactorial phenomenon with a strong spatial variability depending on the pollutant and location type. EU-wide reduction measures can affect both local pollution in hot spots as well as background pollution. To address exceedances in hot spots, local measures will be needed that may differ depending on the area and region of interest. Road transport would still be a primary focus for such emission controls as it is one of the main causes of non-compliance with air quality standards, especially for NO_2. In recent years the NO_x emissions of road transport in Europe were just under 40% of the total NO_x emissions (EEA, 2022, 2021, 2020). Therefore, regulating the emissions of road vehicles would be one of the key instruments. With this goal, on the 10th of November 2022 the European Commission published a proposal for new Euro 7/VII emission standards (European Commission, 2022c). The key change compared to the current Euro 6d standard is for diesel passenger cars and light commercial vehicles having to comply with the same NO_x limit as gasoline cars. To tackle NO_2 pollution also local measures play an important role. A comprehensive list of local measures can be found in the report '*Best practices for local and regional air quality management*' (FAIRMODE, 2022; Pisoni et al., 2022). Specifically, to reduce NO_x emissions from road transport the following measures are listed: low-emission zones; congestion charges; promotion of public transport and cycling; speed limits reduction on highways; and restrictions of heavy traffic. Besides the road transport sector there are other sectors that contribute to NO_x emissions. Also, these sectors are subject to further restrictions. For example, on the 5th of April 2022 the European Commission adopted a proposal to revise the Industrial Emissions Directive (IED) (European Commission, 2022d). To find the right solutions for improving air quality, it is therefore essential to carefully evaluate the contribution to pollutant concentrations of different source categories, when assessing EU-wide and local measures to improve air quality in hotspots. The need for robust regional and local air quality planning requires methodologies that should be adequate to provide detailed and robust information on the sectoral contributions and their associated impacts on air quality.

Several methodologies exist to model the impact of a combination of measures at different policy levels from the European scale to the local street-level scale. Spanning these scales is necessary because exceedances of the limits often occur in busy streets in cities where background emissions from regional traffic and other sectors, combine with local emissions. All methodologies combine low-resolution (typically 4–10 km) chemistry transport models (CTM) with high-resolution (typically 10–100 m) dispersion models. Two examples of such an approach are ATMO-Street and urbanEMEP. The ATMO-Street model chain (Hooyberghs et al., 2022; Lefebvre et al., 2013a) uses low-resolution background concentrations either as predicted by a Chimere (Mailler et al., 2017) CTM run or spatially interpolated measurements with the RIO model (Janssen et al., 2008). High-resolution results are obtained with a combination of a Gaussian plume model (IFDM) and the OSPM street canyon model (Berkowicz, 2000)). The latter two models only calculate the local impact of emissions. Hence, when emission reductions have a large impact over longer distances and influence the background substantially a new CTM run is required. MetNO's urban EMEP or uEMEP (Rolstad Denby et al., 2020) combines the EMEP CTM with a Gaussian dispersion model. The key feature of this methodology is that the CTM keeps track of the local contribution (concentration due to emissions from each grid cell) to the concentration. This local contribution is downscaled at higher resolution (250–50 m) with a Gaussian dispersion model. In this way the consistency between low- and high-resolution modelling is guaranteed. The disadvantage of these model chains is that the CTM-step is slow, running for many hours or days on a high-performance cluster (HPC). They offer an hourly output for a complete year, but often only the impact on the annual average concentration of measures is of interest.

A faster and more flexible model chain that allows for analysis of different combinations of international, national, and local measures is desirable. To calculate the international or national contribution more quickly several approaches have been developed that approximate the CTM by a faster surrogate model. We opted for the SHERPA source-receptor model (Pisoni et al., 2019; Thunis et al., 2016, 2018). SHERPA calculates the change in annual average concentration as a function of distance-weighted emission changes of the relevant precursors. A more detailed explanation follows in section 3. Another approach was chosen by Carnevale et al. (2012), who built a fast surrogate model of a CTM using Artificial Neural Networks. This allowed them to integrate air quality calculations in an optimization to compute the most cost-effective air quality policies. Bessagnet et al. (2019) used machine learning to approximate the CHIMERE CTM so that it can be used for air quality forecasting, analysis of pollution episodes and mapping. The GAINS modelling system (Kiesewetter et al., 2015) uses still another approach that derives source-receptor relations between regions from individual EMEP CTM runs. Also, to speed up the calculations of the local high-resolution contribution to NO_2 concentrations there are several strategies. To develop C-PORT, a screening tool for near-port air quality assessment, (Isakov et al., 2017) simplified to the maximum the underlying plume dispersion model. SHERPA-city, a model developed at the EC's JRC (Degraeuwe et al., 2021), calculates the effects of a LEZ and activity changes on the annual average NO_2 concentration at a 20-m resolution. The calculation time is in the order of minutes because a kernel approach is used. No long-distance impacts of new emission standards or non-traffic measures can be simulated. Due to the limited size of the kernels only the local impact of measures can be determined.

This paper proposes an alternative methodology to model the impact from non-traffic sectors as well as the impact from traffic measures at both EU-wide as well as local level on the NO_2 concentration. In contrast to the models presented above, this alternative methodology is fast and responsive. To reduce the computation time and complexity, only annual average results are calculated; no hourly results to evaluate the exceedance of hourly limits are available. Results are available in a matter of seconds. This is important for source apportionment and planning where one wants to explore various contributions and measures. In this way the methodology is aligned with the requirements of the web-application. With road transport being of particular interest, the application can model the effect of both local measures (e.g., LEZ, access regulations, traffic calming measures) as well as international and national measures (e.g., new emission standards). For this purpose, both the long-distance effects and the strong NO_2 gradients close to roads are modelled. Emissions scenarios for other sectors are also considered, but in less detail than for road transport. The application should be EU-wide but with a particular focus to cities. Therefore, results for the major European cities and air quality monitoring stations within these cities are required.

To this end, we designed a modelling system based on precalculated data. The main idea is that emissions and corresponding concentration

layers that are relevant for the measures to be analysed are calculated in advance. To keep the computational effort low, only annual average impacts are calculated. The long-distance effects are calculated by the SHERPA model (Thunis et al., 2016), while the strong local gradients are calculated by VITO's QUARK model (Quick Urban AiR quality using Kernels): a kernel-based model derived from a Gaussian plume model. A kernel is the annual average NO_x concentration around a road segment. Such kernels were calculated for different orientations of the road (from North-South to East-West in steps of 15°) and for meteorological conditions across the EU27+UK.

The article is structured as follows: In the next section the data are described. Subsection 2.1 describes the emission data used for the low-resolution SHERPA modelling. Subsection 2.2 describes the high-resolution road transport data set. Section 3 is dedicated to the methodology and has a subsection dedicated to the low- and high-resolution modelling. In section 4 some results, and validation statistics are presented. Section 5 discusses the advantages and shortcomings of the methodology.

2. Description of the data

The objective is to develop an EU-wide source apportionment and emissions scenario functionality to predict NO_2 concentrations both in cities and at individual measurement stations. As the modelling application has a particular focus on the traffic sector, more detail regarding the contribution of each individual vehicle type is needed, while for non-traffic sectors we are interested in the contribution of the whole sector. This section describes the necessary data to perform this analysis. Spatial emission data per GNFR[2] sector is needed for a sectorial source apportionment (section 2.1). A high-resolution road network and detailed fleet data are needed to simulate the impact of urban access scenarios and/or a new vehicle emission standard (section 2.2).

2.1. Emissions from non-traffic sectors

The total NO_x emissions per country and GNFR[3] sector of the 2nd Clean Air Outlook (CAO2), available on the GAINS website,[4] were used. The emissions of the following scenarios were used:

- The ***CAO2 baseline*** scenario includes the latest EU-wide legislation and already adopted national pollution control measures. Available years: every 5 years from 2015 to 2050. The CAO2 baseline is also used as the baseline scenario in the application.
- *The* ***CAO2 baseline*** + ***MTFR*** scenario includes the maximum technically feasible reductions. Available years: 2030 and 2050.
- The ***NAPCP*** (National Air Pollution Control Programmes and Projections.) scenario also includes additional measures selected for adoption. Available years: every 5 years from 2015 to 2050.
- The ***1.5 LIFE*** + ***MTFR*** scenario includes both the 1.5 LIFE climate scenario and maximum technically feasible reductions. Available for 2050.

In total, 19 scenario-year combinations were included in the application. A more detailed description of the different scenarios can be found in the CAO2 report (Amann et al., 2020). To use these national total emissions per sector for source apportionment calculations with SHERPA, they must be spread on a grid. Therefore, the CAMS[5] gridded emissions of 2018 were used as proxy because they have the same resolution as the SHERPA-model: 0.1-by-0.1°. The CAMS data were downloaded from the CAMS Atmosphere Data Store.[6]

2.2. High-resolution road transport emissions

To model the NO_2 concentrations from road transport at high resolution, a dataset with the traffic intensity on each road is needed. Such a dataset does not exist at European level. Therefore, we developed the EU Traffic Data Mapper (ETDM). The ETDM spreads the national total vehicle kilometres over the road network with a proxy based on the population and road capacity. Emissions on each road segment are calculated taking into account the traffic composition.

National vehicle kilometres and emissions data is available in the Sybil tool developed by EMISIA.[7] Traffic data is provided per country, per vehicle type (a combination of vehicle category, segment, fuel type, Euro standard and age) and road type (urban, rural and highway). The location of the roads comes from OpenStreetMap (OSM) (OpenStreetMap contributors, 2023). For computational reasons this network had to be simplified with a tolerance of 50 m. To allocate a fleet to each road with the correct share of heavy and light traffic, each road link had to be identified as a *highway*, *rural* or *urban road*. All roads of the type '*mainRoad*' in the OSM data are labelled as *highway*. All other roads are either classified as urban or rural based on the Global Human Settlement Layer (GHSL) (https://ghsl.jrc.ec.europa.eu/). Roads located in '*urban clusters*' (low-density clusters) and '*urban centres*' (high-density clusters) are labelled *urban*. The remaining roads are labelled *rural*.

To spread national vehicle kilometres, a proxy was defined using the population density around each road and the road capacity. The population was taken from the GHSL; the road capacity was retrieved from OpenTransportMaps (OTM) (Jedlicka et al., 2015). OTM provides traffic volume and road capacity estimates. Here the capacity estimates were used to construct the following weight *w*:

$$w = l \bullet ln(pop_{50km}) \bullet C \quad \text{Eq. 1}$$

C is the capacity attribute of the road in the OTM data set, *l* is the length of the road and pop_{50km} is the population in a 50-by-50-km square around the location of the road. The total highway and combined urban and rural vehicle kilometres per country are subsequently spread over the roads according to the weights defined above. For each road, the vehicle kilometres on the road are defined as the country total vehicle kilometres for the road type multiplied by the ratio of the weight of the road to the weight summed over the roads of the same class. The vehicle kilometres for each road are then divided by the length of the road to obtain the daily mean number of vehicles for each road segment. A similar approach using OTM and population as a proxy was used by Kuenen et al. (2022). A comparison between the ETDM dataset and regional traffic dataset for Flanders, Belgium, can be found the Annex 10.3 Validation of the traffic data set.

In this way, the ETDM tool can generate a database with EU-wide traffic intensities at each road segment. These are subsequently fed to the FASTRACE emission model to generate the actual traffic emissions in kg/km/h for each road segment. FASTRACE (Hooyberghs et al., 2022) is a software tool developed by VITO to calculate spatially disaggregated emissions from road transport, starting from country specific vehicle fleet data, COPERT emission factors (Ntziachristos et al., 2020) and traffic intensities at the street level. FASTRACE calculates the emission per vehicle type and per road segment as follows:

[2] General Nomenclature for Reporting [of emissions] used by the European Environment Agency (EEA).

[3] The GNFR sectors considered in the web-application are: GNFR A: Power Generation, GNFR B: Industry, GNFR C: Ohter Stationary Combustion (e.g., domestic heating), GNFR F: Road Transport, GNFR G: Shipping, GNFR H: Aviation, GNFR I: Offroad, GNFR J: Waste, GNFR K: Livestock, GNFR L: Other Agriculture.

[4] https://gains.iiasa.ac.at/gains/EUN/index.login?logout=1&switch_version=v0.

[5] CAMS: Copernicus Atmosphere Monitoring Services, https://atmosphere.copernicus.eu/.

[6] https://atmosphere.copernicus.eu/data.

[7] https://www.emisia.com/utilities/sibyl-baseline/.

$$E_{vrp} = vkm_{vr} \bullet EF_{vtps} \quad \text{Eq. 2}$$

where E_{vrp} are the emissions of vehicle type v on road segment r for pollutant p [kg], vkm_{vr} are the total number of vehicle kilometres driven by vehicles of type v on road segment r [km] and EF_{vtps} is the emission factor for pollutant p for vehicle type v and road type t and speed s [kg/km]. The emission factors are road type and speed dependent, based on the country specific COPERT 5 emission factors.

To make the definition of scenarios easier for the user the over 400 vehicle types were aggregated to 42 types. Some older emission standards (e.g., pre-euro 1 to Euro 3) are lumped together because they represent only a small fraction of the fleet. More detail about the aggregation can be found in Annex 10.1. Hence, the result of this data preprocessing is 42 road maps with traffic intensities and emissions in the EU27+UK every 5 years from 2015 to 2050. For the different CAO2 scenarios of the same year the national total vehicle kilometres were scaled to match the CAO2 scenario. The detailed fleet composition of Sybil was kept unchanged because the CAO2 traffic data do not provide the high level of detail needed to model urban access scenarios.

This application also includes a functionality that allows exploring the impact of a not-yet-defined[8] Euro 7/VII standard to be introduced on the 1st of January 2027 for diesel and petrol passenger cars, diesel and petrol light duty vehicles and diesel trucks. Therefore, all respective Euro 6, Euro 6d or Euro VI vehicles built in 2027 or later were labelled as Euro 7 or Euro VII. By default, they have the same emission factors as their Euro 6d/VI counterparts. But by having separate emission and concentration layers for these vehicles, the layer can be multiplied with a reduction factor to simulate the effect of different new standards with reduced emissions.

2.3. Urban areas

The objective of the application is to define traffic measures at the level of European cities. Thus, the geographical boundaries of the cities must be defined. For this purpose, our choice was not the currently existing low-emission zones but a larger set of urban areas. This resulted in the use of the spatial units of Eurostat. Eurostat[9] defines three types of urban entities: *Cities*, *Greater Cities*, and *Functional Urban Areas*; a *City* is an administrative unit with more than 50.000 inhabitants, a *Greater City* consists of a city and its commuting zone, a *Functional Urban Area* approximates the urban centre when this stretches far beyond the administrative city boundaries. The *Cities* and *Greater Cities* as defined by Eurostat are similar or somewhat bigger than the typical low-emission zones (LEZ). The Eurostat *Functional Urban Areas* are too big compared to typical LEZ. Therefore, only the *Cities* and *Greater Cities* were selected. This results in 948 cities, as defined by Eurostat, in the EU27+UK. For each city the Eurostat polygon was used to select the roads from the road network to create a layer with urban emissions for each vehicle type. The polygon was also used for the SHERPA source apportionment per sector to determine the contributions of each sector originating from inside or outside the city.

2.4. Other data

As reference concentration map, the CAMS NO_2 ensemble of 2018 was used from the CAMS Atmospheric Data Store.[10] This is the median concentration of 8 CTMs and can be considered as the best available model estimate. To produce the high-resolution kernels for the QUARK model, ECMWF weather data from 2015 were used. For the compliance module the 3136 stations in the EU27+UK available on the European Environment Agency's Air Quality e-reporting website were used (See Annex 10.2 for the query used to retrieve the data).

3. Methodology

This section explains the steps taken to develop the methodology to calculate the NO_2 concentration at a measurement station or a concentration map for a city (Fig. 1) for a given scenario. First the low-resolution NO_x contribution of each GNFR sector is calculated with the SHERPA source apportionment model. In the case of a measurement station the contribution of each sector is calculated. In the case of a city, the sector contributions from both inside and outside the city are calculated. This is explained further in section 0. The second step is the calculation of the high-resolution NO_x contributions from 42 vehicle types with the QUARK kernel dispersion model. A double-counting correction is necessary because traffic emissions are already included in the low-resolution calculations. A detailed explanation follows in section 3.2. In the third step the NO_x concentrations are converted to NO_2 concentrations with an empirical correlation (section 3.3). In the last step a bias correction is applied (3.4). The bias was derived from a comparison with observations in 2018. Eq. (3) shows the general outline of the calculation. High-resolution contributions of various areas and sectors ($[NOx]_{area,sector}$) are weighted (weights w) according to the user-defined scenario and summed. This sum is converted to an NO_2 concentration with an empirical correlation (f_{NO2}). For every station (i) a relative bias correction ($C_{bias,i}$) is applied based on the observations of 2018. The bias correction can only be applied to the measurement stations, not to the city maps.

$$[NO_2] = C_{bias,i} \bullet f_{NO2}\left(\sum_{area}\sum_{sector} w \bullet [NO_x]_{area,sector}\right) \quad \text{Eq. 3}$$

3.1. Low-resolution sectorial and spatial source apportionment with SHERPA

For each sector-area combination, the contribution is determined with the SHERPA model (long-distance low-resolution impacts in Fig. 1). SHERPA is a source-receptor model that approximates a full Chemistry Transport Model (Pisoni et al., 2019; Thunis et al., 2016). SHERPA allows for flexible source apportionments calculations. It is possible to determine the impact of the sectoral emissions of any area, represented by a group of CTM cells, on the concentrations in any other area. More specifically it a) determines the contribution of a sector to the concentration in a given point (e.g., the contribution of the industrial sector on a specific measurement station), b) determines the contribution of a sector to an area, represented by a group of cells (e.g., the contribution of the shipping emissions on the concentrations in a city) or c) determines the contribution of a sector in specific area of interest to a group of cells (e.g., the contribution of the traffic emissions inside a city on the concentrations in the same city). The concentration change in a cell due to emission changes in the surroundings is calculated with the following formula (Pisoni et al., 2017):

$$\Delta[NO_x]_j = \alpha_j^{NOx} \bullet \sum_i \left(1 + d_{ij}\right)^{-\alpha_j^{NOx}} \bullet \Delta E_i^{NOx} \quad \text{Eq. 4}$$

In which:

j: the receptor grid cell where the concentration change is calculated. In this case it is a cell in which a measurement station is located or a cell inside a city polygon.

i: cells around the receptor cell j whose emissions changes are considered to calculate the concentration change in cell j. Emissions in grid cells within a radius of 140 cells around the receptor cell are considered.

$\Delta[NO_x]_j$: the NO_x-concentration changes in the receptor cell j

[8] At the moment of writing the article, the Euro 7/VII standard was not yet defined. The introductory year is assumed to be 1st of January 2027.

[9] Eurostat, what is a city? - Spatial units: https://ec.europa.eu/eurostat/web/cities/spatial-units.

[10] https://atmosphere.copernicus.eu/data.

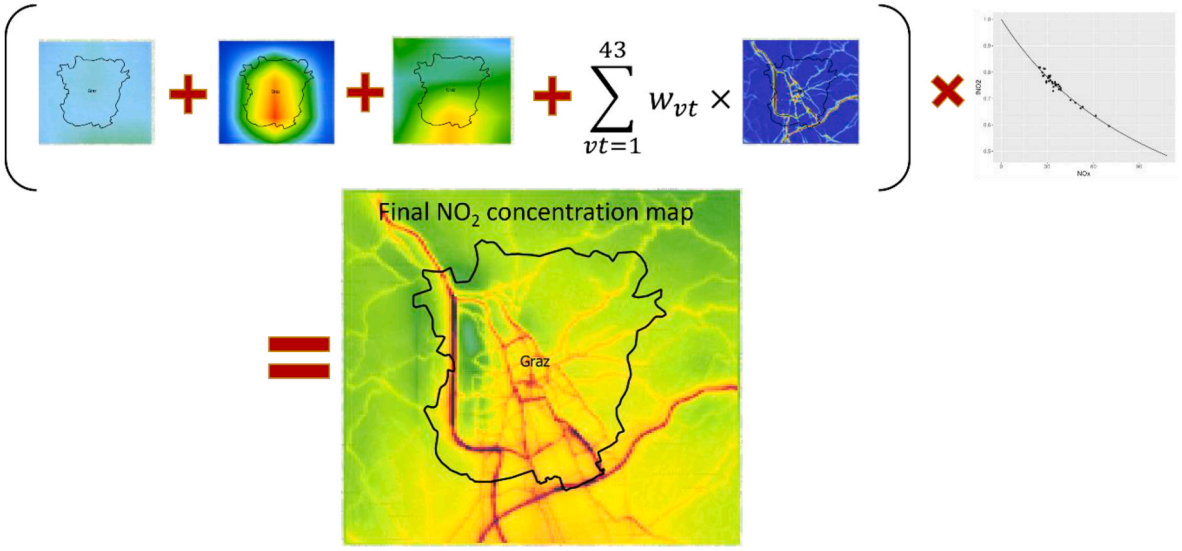

Fig. 1. Summary of the methodology to calculate the NO_2 concentration map for a city.

ΔE_i^{NOx}: the NO_x emission changes in cells *i*.

d_{ij}: the distance (in grid cells) between the source cells *i* and the receptor grid cell *j*.

α_j^{NOx}: represents the impact of NO_x emissions in cell *j* on the NO_x concentration in the same cell. The unit is $\mu g/m^3/kton$. Values are high when atmospheric conditions are more stable and wind speeds are low.

ω_j^{NOx}: width of the source-receptor relationship for cell *j*, high values indicate a more localized impact of the emissions.

In this way SHERPA considers the long-distance impact of measures, admittedly at the resolution of a typical Chemistry Transport Model (CTM) of about 10-by-10 km. For all contributions of interest (sectors inside and outside each city) the SHERPA model was run with emissions reductions of 100%, i.e., the reduction is equal to the total emissions ($\Delta E_i^{NOx} = E_i^{NOx}$). SHERPA is an approximation for small emission changes (up to 50%) around a reference case. However, for NO_x the model is well capable of predicting the full concentration column quite accurately. Because Eq. (4) is linear in the emissions, the resulting concentrations are proportional to the emission reduction. These calculations result in NO_2 contributions per sector and area ($[NO_2]_{area,sector}^{SHERPA}$) in the case of a city and contributions per sector ($[NO_2]_{sector}^{SHERPA}$) in the case of an air quality station. The sum of all sector area contributions ($[NO_2]^{SHERPA}$) is calculated as the sum over all sectoral and area contributions:

$$[NO_2]^{SHERPA} = \sum_{area}\sum_{sector} [NO_2]_{area,sector}^{SHERPA} \quad \text{Eq. 5}$$

For the year 2018 a calibration factor is derived to adjust for the difference between the SHERPA result ($[NO_2]_{2018}^{SHERPA}$) and CAMS 2018 NO_2 ensemble, which is considered the best available estimate of the annual average NO_2 concentration. This calibration factor has a geometrical mean of 1.12 (relative standard deviation of 14%) for the 948 cities considered in the application. This calibration factor is applied to all CAO2 scenarios and years.

$$f_{calib2CAMS} = [NO_2]_{2018}^{CAMS} / [NO_2]_{2018}^{SHERPA} \quad \text{Eq. 6}$$

Each NO_2 contribution is converted to a NO_x contribution by multiplying it with a NO_x/NO_2-ratio. This ratio is obtained by applying the inverse of the Bächlin correlation, f_{NO2}^{-1}, on the total calibrated NO_2 column and dividing it by the total calibrated NO_2 as shown in Eq. (7).

$$[NO_x]_{area,sector}^{SHERPA} = [NO_2]_{area,sector}^{SHERPA} \bullet f_{calib2CAMS} \bullet \frac{f_{NO2}^{-1}\left([NO_2]^{SHERPA} \bullet f_{calib2CAMS}\right)}{[NO_2]^{SHERPA} \bullet f_{calib2CAMS}} \quad \text{Eq. 7}$$

The Bächlin correlation (Bächlin et al., 2008), f_{NO2}, is an empirical correlation between the annual average NO_2 and NO_x concentration and is given by:

$$[NO_2] = \frac{A \bullet [NO_x]}{[NO_x] + B} + C \bullet [NO_x] \quad \text{Eq. 8}$$

With $A = 29$, $B = 35$ and $C = 0.217$

When solving Eq. (8) for NO_x it gives the inverse Bächlin correlation, f_{NO2}^{-1}, which expresses annual average NO_x as a function of annual average NO_2:

$$[NO_X] = \frac{-\left(A + B \bullet C - [NO_2] + \sqrt{D}\right)}{2 \bullet C} \equiv f_{NO2}^{-1}([NO_2]) \quad \text{Eq. 9}$$

$$with\ D = (A + B \bullet C - [NO_2])^2 + 4 \bullet B \bullet C \bullet (A + B \bullet C - [NO_2])$$

In this way we have created artificial NO_x contributions (Eq. (7)) that will be converted back to NO_2 after summing them with weights according to the user defined scenario. The weights of the non-traffic sectors in Eq. (3) are values between 0 and 1 chosen by the user. Because for traffic there are more options (e.g., defining a Euro 7 emission standard and defining urban access regulations) the calculation of the weights is more complex. The weight of low-resolution traffic contribution from outside the city, $w_{OutCity,Traf}$, is calculated as follows:

$$w_{OutCity,Traf} = f_{NonE7} + \sum_{E7} f_{E7} \bullet r_{E7} \quad \text{Eq. 10}$$

where f_{NonE7} is the fraction of NO_x emissions due to non-Euro7 vehicles. f_{E7} is the fraction of NO_x emissions in a country for a given year due to one of the five Euro 7 vehicle types. r_{E7} is the reduction of the emission factor for one of the five Euro 7 vehicle types defined by the user. The weight for the contributions inside the city, $w_{InCity,Traf}$, is calculated as follows:

$$w_{InCity,Traf} = \sum_{vt} f_{vt} \bullet r_{E7} \bullet r_{UrbAcc} \quad \text{Eq. 11}$$

where f_{vt} is the fraction of NO_x emissions in a country for a given year due to one of the 42 vehicle types. r_{E7} is 1 for non-Euro7 vehicle types or the user defined reduction. r_{UrbAcc} is the change in emissions due to

urban access regulations. When a vehicle type is banned, its weight is zero. When some types of a category (passenger car, light duty vehicle, trucks) are banned, it is assumed that the associated vehicle kilometres are proportionally attributed to the remaining allowed types. The user can also increase or decrease the vehicle kilometres and corresponding emissions of individual vehicle types. These adjustments to the base case are contained in the factor r_{UrbAcc}.

3.2. High-resolution concentrations with the QUARK kernel method

To calculate the contribution to the NO_x and NO_2 concentrations from different vehicle types at high resolution, the QUARK high-resolution methodology was applied (high-resolution impact of 42 vehicle types in Fig. 1). QUARK stands for Quick Urban AiR quality modelling using Kernels (Maiheu et al., 2017). The method is based on a database of dispersion patterns which were pre-computed using the IFDM Gaussian Dispersion model (Lefebvre et al., 2013b) for a line source of 100 m with an emission strength of 1 kg/km/hour. There are separate dispersion patterns for different orientations of the line source with respect to the north-south axis (in 10° steps). Separate kernels were computed in areas with distinctly different meteorology; for more details we refer to the (Maiheu et al., 2017) report. Fig. 2 below illustrates the different annual concentration patterns obtained in different locations using the same unit line source. The meteorological data used for these kernels is based on ECMWF ERA-Interim data for 2015.

In the QUARK methodology, the unit dispersion patterns are subsequently scaled with the emission strengths per vehicle type on each line segment of the road network and summed. This results in NO_x concentration maps per vehicle type. The size of the kernels is limited (± 4 km × 4 km). This is large enough to capture the strong gradients around roads. However, this local effect is already considered by the SHERPA source-receptors (together with the long-distance effect). Therefore, the QUARK contribution cannot be directly summed to the SHERPA contribution. To avoid double counting a moving average window of the same size as the kernel is swept over the QUARK rasters and subtracted from the original. When this raster is added to the SHERPA contribution its net contribution is zero (no double-counting) but the gradients around roads are included. This results in NO_x concentration maps per vehicle type with double counting correction in a specific area ($[NO_x]^{QUARK}_{area,vt}$). These contributions are weighted and summed over all vehicle types to result in the local traffic contribution: $[NO_x]^{QUARK}_{area,Traf}$. Eq. (12) shows the local traffic contribution inside a city. The weights in Eq. (12) are the same as in Eq. (11), and determined by the user defined Euro7 standard and the urban access regulations.

$$[NO_x]^{QUARK}_{InCity,Traf} = \sum_{vt} [NO_x]^{QUARK}_{InCity,vt} \bullet r_{E7} \bullet r_{UrbAcc} \quad \text{Eq. 12}$$

Specifically for traffic inside a city, the NO_x contribution in Eq. (3) becomes:

$$[NO_x]_{InCity,Traf} = w_{InCity,Traf} \bullet [NO_x]^{SHERPA}_{InCity,Traf} + [NO_x]^{QUARK}_{InCity,Traf} + w_{OutCity,Traf} \bullet [NO_x]^{SHERPA}_{OutCity,Traf} + [NO_x]^{QUARK}_{OutCity,Traf} \quad \text{Eq. 13}$$

For the calculations at measurement stations the distinction between inside and outside a city does not apply, but the QUARK traffic contribution with double counting correction is used in the same way.

3.3. Conversion of annual average NO_x to NO_2

How the annual average NO_x concentrations translate to an annual average NO_2-concentrations depends mainly on the fast chemical reactions between nitrogen oxides, volatile organic compounds, and ozone. In a CTM (Simpson et al., 2012) or a Gaussian dispersion model (Lefebvre et al., 2013a) this interplay can be considered at hourly or higher frequency. However, here only annual average NO_x and ozone are available. There are two options to convert the annual average NO_x into NO_2: using empirical correlations or modelled values. The empirical correlations like the ones of Düring, Romberg or Bächlin (Bächlin et al., 2008) predict the observed trend between annual average NO_x and NO_2 very well, as shown for the AQ e-reporting observations of 2018 in Fig. 3. However, there is a significant scatter, while the relative RMSE is 13%. Typically, most of the NO_x occurs as NO_2 when NO_x-concentrations are low and with increasing NO_x concentrations the NO_2 fraction decreases to 50% or lower. Consequently, the effect of emission

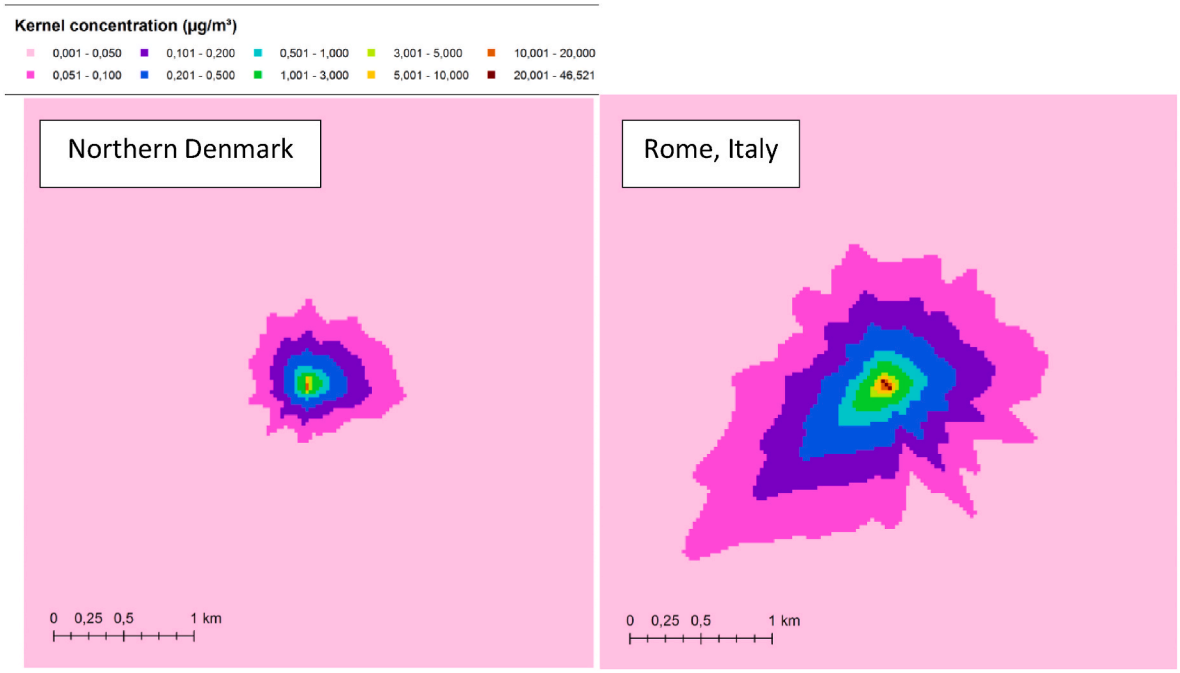

Fig. 2. Left - annual average dispersion kernel for a 100 m line source of emission strength 1 kg/km/hour, at an angle of 5° from the North-South axis in the Northern part of Denmark. Right - Kernel for a 100m line source, of emission strength 1 kg/km/hour, at an angle of 135° from the North-South axis slightly north of Rome, Italy.

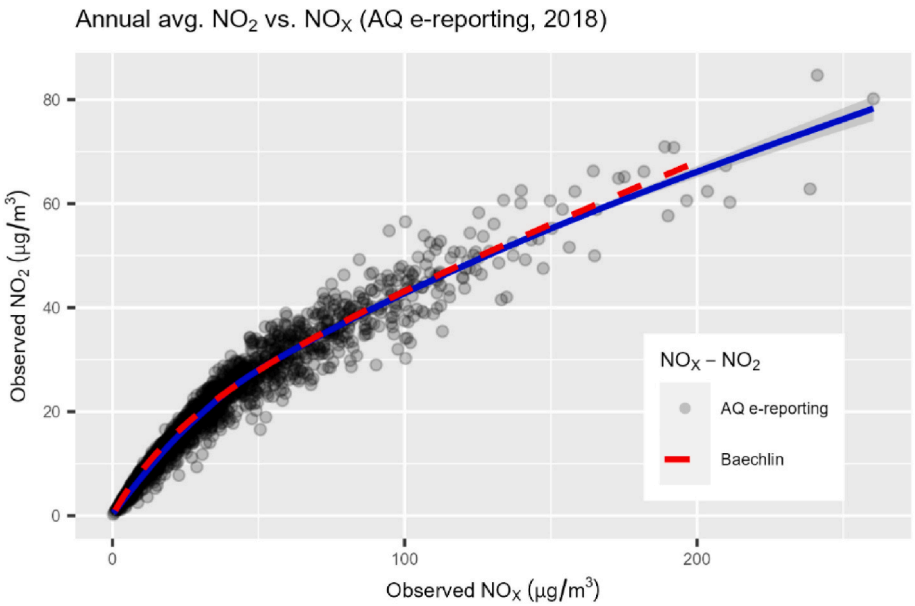

Fig. 3. Comparison between observed annual average NO_x –NO_2 pairs (grey dots) and the Bächlin correlation (red line). The blue line is a trend line through the observations.

reductions on the NO_2 concentrations is counteracted to a certain extent by a shift from NO to NO_2 (titration effect). The other model-based option would be to use the NO_2 fraction predicted by the CAMS ensemble. Fig. 4 shows a comparison between the NO_2 fraction from observations in 2018 (AQ e-reporting) and the CAMS ensemble. The correlation is very low even for background stations. So, this is not a good option to convert annual average NO_x into NO_2.

The goal is to get the NO_2 concentration right. Hence, for this application we converted the NO_2 contributions of different sectors in NO_x with the inverse Bächlin correlation. After applying a weighted sum of the NO_x contributions according to the desired scenario the result is converted back to NO_2 ($NO_x \rightarrow NO_2$ in Fig. 1). In this way no extra error is introduced because of the scatter around the Bächlin correlation, and the titration effect is considered.

3.4. Bias correction

For the measurement stations a bias correction is also applied. For each station the relative bias was determined between the observed and modelled value in 2018. This ratio is multiplied with the model result for every CAO2 scenario-year combination (see Eq. (3)). This bias correction is especially important for traffic stations in street canyons. The model does not take street canyons into account, which is the main cause of a considerable underestimation of the concentrations of −18.1 µg/m^3 (see section 4 on validation). The absence of the street canyon effect is the major but not the only cause of the negative bias (underprediction). However, it could not be modelled because both accurate traffic data and street canyon geometries are not available for each canyon. Applying a bias correction gives more realistic concentrations but the results must be interpreted with care. The increased concentration in canyons is due to traffic pollution trapped in the street. Hence, the street

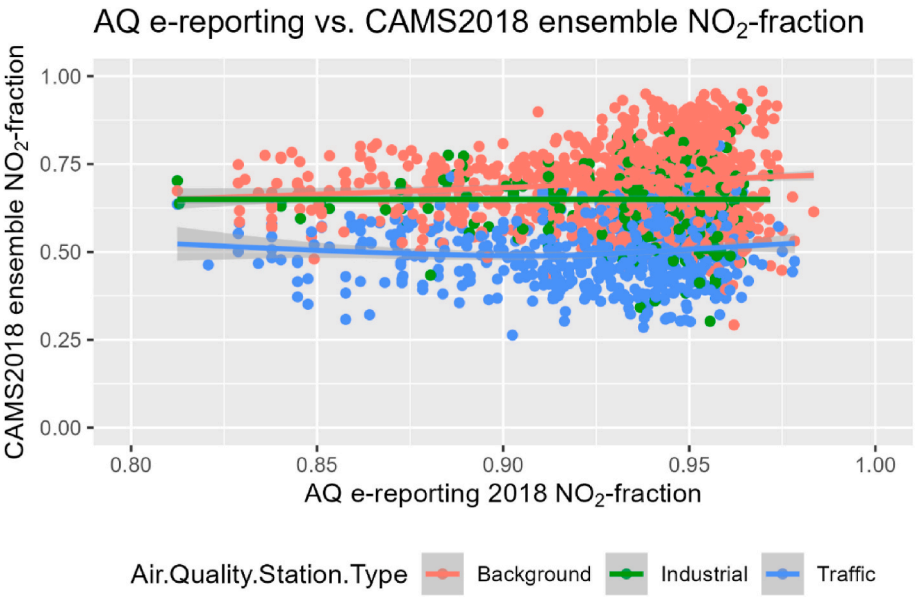

Fig. 4. Comparison between observed (Air Quality e-reporting) and modelled (CAMS, 2018 ensemble) annual average NO_2 fraction per station type.

canyon effect is proportional to the emissions in the canyon. This means that if in a user-defined scenario traffic emissions are modified also the bias correction should be modified. But how much this correction should change can only be determined by explicitly modelling the canyon effect.

4. Results and validation

Fig. 1 shows how the steps described in Section 3 are used to create an NO_2 concentration map for the city of Graz, Austria. First, the total NO_x concentration is calculated by summing the following contributions: 1) the sum of nine non-traffic sectors multiplied by their respective weights defined by the user; 2) the long-distance, low-resolution contribution from traffic inside the city calculated with SHERPA and adjusted for emission changes due to the user-defined access regulations and Euro 7 standard; 3) the long-distance, low-resolution contribution form traffic outside the city calculated with SHERPA and adjusted for emission changes due to the user-defined Euro 7 standard; 4) the high-resolution contribution from traffic outside the city with double-counting correction calculated with QUARK and adjusted for the user-defined Euro 7 standard and 5) The high-resolution contribution from traffic inside the city with double-counting correction calculated with QUARK and adjusted for the user-defined access regulations and Euro 7 standard. These resulted in the generation of 42 layers, with an additional 43rd layer for the high-resolution traffic outside the city. This total NO_x concentration is converted to NO_2 with the Bächlin correlation. Fig. 5 shows an example of the concentrations calculated at station level with only the power generation and industrial sector switched on. It gives an overview of where in Europe these sectors contribute the most to the NO_2 concentration. More examples will be presented in a dedicated publication that is under preparation.

The results of the CAMS + SHERPA + QUARK model chain was validated against the AQ e-reporting observations of 2018. Because the CAO2 does not have data for 2018, a linear interpolation between 2015 and 2020 baseline was used. Table 1 shows the results. The first row shows bias, RMSE and Pearson R^2 for all 3.136 stations in the EU27+UK. The first three columns show the validation characteristics for the CAMS 2018 ensemble only. The next three columns show the validation statistics for the whole model chain without bias correction. By adding the SHERPA and QUARK traffic contribution the bias decreases from −9.9 to −9.1 μg/m^3, the RMSE decreases from 14.0 to 13.0 μg/m^3 and the Pearson correlation increases from 0.60 to 0.68. Table 1 also shows the validation statistics per station type (background, industrial and traffic) and further per station area (rural, suburban, and urban). Hence, adding the high-resolution traffic reduces bias and RMSE, and increases the Pearson R^2. But also, with high-resolution traffic the average bias remains negative. Non-road transport sectors are still treated at low resolution, this spreads the impact uniformly over a CTM cell and ignores local gradients close to the source. When high resolution data for other sectors are available, the same methodology as for traffic can be applied to increase the accuracy. At traffic stations there is a very important negative bias (underestimation), this is mainly because the street canyon effect is not considered. This is the main reason why a bias correction was introduced as explained in section 3.4. In the web-application all data are available for download and the bias correction is available separately. Hence, the user can evaluate the effect of the correction.

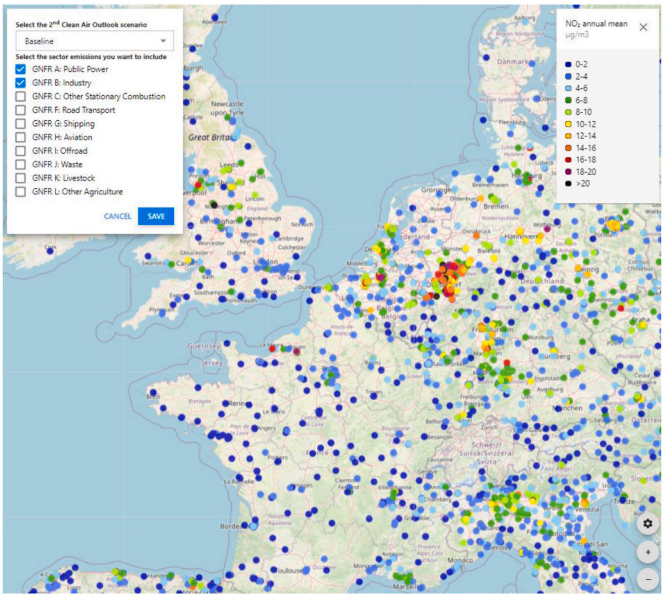

Fig. 5. Contribution of the public power sector (GNFR A) and the industry (GNFR B) in 3.136 measurement stations for the CAO2 baseline scenario 2030.

5. Discussion and conclusion

In this paper we have presented a novel methodology for NO_2 source apportionment. Both the long-distance impact as the local impact close to roads are considered by using a combination of the SHERPA source-receptor model and the QUARK kernel model. The main advantage over modelling with a CTM is that for a wide range of scenarios both concentrations at air quality stations and concentration maps for cities can be calculated in a matter of seconds. Because of the speedy calculations it is possible to integrate this methodology in a responsive NO_2 source apportionment web-application. This web-application and some examples will be described in a dedicated follow-up publication. To achieve short calculation times some concessions had to be made. The method only gives results for the annual average concentrations. The results are obtained by combining pre-calculated data, which limits to some extent the scenarios a user can define. While non-traffic sectors can only be switched on or off, special attention is given to the road transport sector, where the application allows the user to study the impact of several scenarios: the impact of a new vehicle emission standard (Euro 7/VII) and urban access regulations modifying the activity of the 42 vehicle types in 948 European cities.

The modelled NO_2 concentrations at 3136 stations were compared with observations. Generally, the model and observations align well, except in traffic stations located in street canyons. Street canyons cannot be included because the necessary data, traffic intensities and canyon geometries, are not available for all stations. Therefore, the model underestimates the concentrations in street canyons. As a solution we opted to correct the modelled concentrations with the relative bias in 2018. Such a correction adjusts the contribution of each sector proportionally. This leads to more realistic results, but they need to be interpreted with care. For instance, in the case of a street canyon, applying a bias correction is justifiable if only emissions of sectors outside road transport are modified. Conversely, if a scenario aims to reduce road transport emissions, the bias correction will lead to an overestimation because it is based on higher road transport emissions.

Another source of uncertainty is the resolution. For computational reasons the high resolution was limited to 100 m. To fully capture the gradients around roads ideally a 10 m resolution would be needed. However, a 10 m resolution would multiply the calculation times by a factor 100, resulting in the application being less responsive. This is a compromise to keep the web-application fast and user-friendly.

The results also depend on the CTM from which the SHERPA model is derived. A source apportionment analysis for PM2.5 with two SHERPA models, one based on the CHIMERE CTM, and another based on the EMEP CTM, showed that most of the time the results are consistent but sometimes differences can occur (Degraeuwe et al., 2020). Repeating this analysis with a source-receptor model based on another CTM might lead to somewhat different results in some cities. But the conclusions relevant for policy makers, i.e., which sector's emissions must be tackled

Table 1
Validation statistics (Bias, RMSE, Pearson R^2) for all air quality stations together, per station type and per country.

AQ Station		CAMS 2018 ensemble			CAMS + SHERPA + QUARK			n
Area	Type	Bias [μg/m^3]	RMSE [μg/m3]	R^2	Bias [μg/m3]	RMSE [μg/m3]	R^2	
all	all	−9.9	14.0	0.60	−9.1	13.0	0.68	3.136
all	Background	−4.8	7.1	0.76	−4.6	6.9	0.77	1.720
all	Industrial	−5.7	8.0	0.69	−5.3	7.6	0.72	395
all	Traffic	−20.1	22.3	0.58	−18.1	20.4	0.60	1.021
Rural	Background	0.1	2.4	0.89	0.1	2.4	0.88	437
Suburban	Background	−4.5	6.5	0.70	−4.2	6.2	0.72	433
Urban	Background	−7.5	8.8	0.76	−7.2	8.6	0.76	850
Rural	Industrial	−2.6	4.7	0.83	−2.5	4.7	0.83	102
Suburban	Industrial	−5.6	7.3	0.75	−4.9	6.6	0.79	180
Urban	Industrial	−8.7	10.9	0.54	−8.3	10.5	0.57	113
Rural	Traffic	−20.0	21.9	0.42	−14.0	17.0	0.46	14
Suburban	Traffic	−15.9	18.8	0.42	−12.7	15.5	0.59	84
Urban	Traffic	−20.5	22.5	0.59	−18.6	20.8	0.61	923

Table 2
42 vehicle types considered for urban access configurations.

Vehicle Category	Fuels	Euro standards
Passenger cars	Diesel	Pre-Euro 4, Euro 4, Euro 5, Euro 6, Euro 6d-TEMP, Euro 6d, **Euro 7**
	Petrol	Pre-Euro 4, Euro 4, Euro 5, Euro 6, **Euro 7**
	CNG	Pre-Euro 4, Euro 4, Euro 5, Euro 6
	Electric	all
Light Duty Vehicles	Diesel	Pre-Euro 4, Euro 4, Euro 5, Euro 6, Euro 6d-TEMP, Euro 6d, **Euro 7**
	Petrol	Pre-Euro 4, Euro 4, Euro 5, Euro 6, **Euro 7**
Two-wheelers	all	all
Heavy Duty Vehicles	Diesel	Pre-Euro IV, Euro IV, Euro V, Euro VI, **Euro VII**
	Petrol	all
Busses	Diesel	Pre-Euro IV, Euro IV, Euro V, Euro VI
	CNG	Pre-Euro IV, Euro IV

to reduce pollution, will remain the same.

The impact sectors, other than road-transport, is more uncertain because the data are considered at the lower resolution of the CTM. Therefore, the contributions of non-traffic sectors are somewhat diluted and not located exactly at the emission sources. This concerns emissions of ships, diesel trains and airplanes. Because the emissions of these sectors, in contrast to road transport, are only important in a limited number of cities, they were not included in the high-resolution modelling. It could be considered as a future improvement.

CRediT authorship contribution statement

Bart Degraeuwe: Writing – original draft, Software, Methodology, Conceptualization. **Hans Hooyberghs:** Data curation. **Stijn Janssen:** Supervision, Conceptualization. **Wouter Lefebvre:** Software, Methodology. **Bino Maiheu:** Software, Methodology. **Athanasios Megaritis:** Writing – review & editing, Conceptualization. **Marlies Vanhulsel:** Data curation.

Declaration of competing interest

The authors declare the following financial interests/personal relationships which may be considered as potential competing interests: Bart Degraeuwe reports financial support and writing assistance were provided by Concawe. If there are other authors, they declare that they have no known competing financial interests or personal relationships that could have appeared to influence the work reported in this paper.

Data availability

A link to a github repository with code and data is available in the Software and data availability section.

Acknowledgements

The QUARK methodology was developed within the project "Improved Methodologies for NO_2 Exposure Assessment in the EU (No. Report nr. 2017/RMA/R/1250)" for the European Commission. The development of the NO_2 source-apportionment application and this publication were supported by funding of Concawe.

Annexes

Vehicle types

The EMISIA data split up the fleet of each country in more than 400 vehicle types or combinations thereof.

- Vehicle category: passenger cars, light commercial vehicles, busses, heavy duty vehicles, L-category
- Fuel: petrol, diesel, CNG, LNG, biofuels, hydrogen, electricity.
- Segment: depends on the vehicle category, small/medium/large size of passenger cars, weight classes for heavy duty vehicles[
- Euro standard: from pre-Euro standard vehicles to Euro VI/Euro 6d

To make the definition of scenarios easier for the user the over 400 vehicle types were aggregated to the 42 types listed in Table 2.

Air quality e-reporting data

https://discomap.eea.europa.eu/App/AirQualityStatistics/index.html?AirPollutant=NO2&ReportingYear=2018&DataAggregationProcess=A

nnual mean/1 calendar year&SourceDataFlow = E1a/validated data AQ e-Reporting&DataCovFilterYN=Yes&potentialOutlier = No.

Validation of the traffic data set

For the region Flanders, Belgium, we compared the EU Traffic Data Mapper (ETDM) with the regional traffic dataset, *Flowmove*. This dataset can be considered as the best available traffic dataset for Flanders, based on traffic counts and modelling. Fig. 6 shows the difference between both traffic datasets around Brussels on a map. The Flowmove network includes many more small roads with little traffic. The total amount of vehicle kilometers in Flanders in both datasets is similar. This implies that in the ETDM dataset vehicle kilometers of smaller roads are transferred to bigger ones.

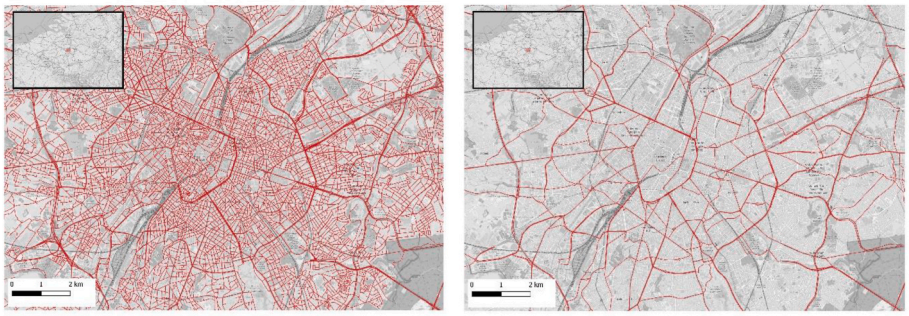

Fig. 6. The road network around Brussels (Belgium) in the Flowmove dataset (left) and the simplified ETDM dataset (right).

Both datasets were also compared at different spatial aggregation levels. Yearly vehicle kilometers were summed per cell for both datasets. Cell sizes of 100-by-100 m, 1000-by-1000 m, 5000-by-5000 m and 10000-by-10000 m were used

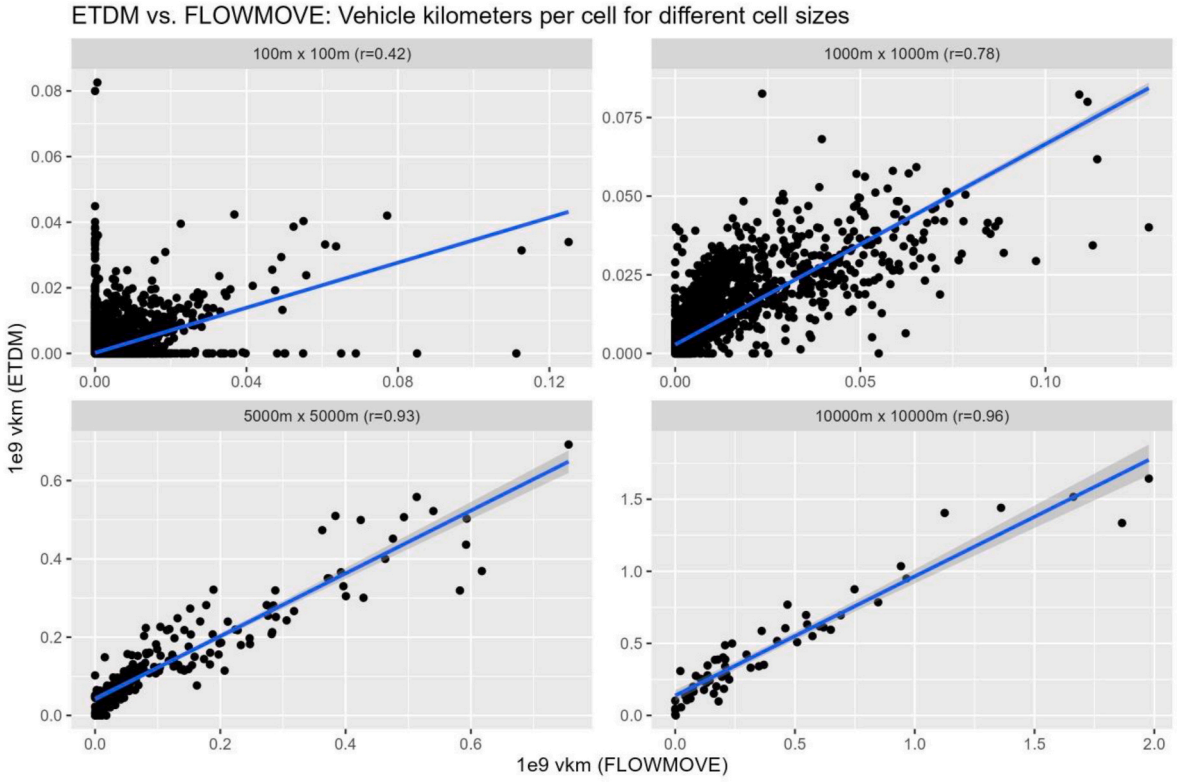

Fig. 7. Comparison of the vehicle kilometers driven per cell for the ETDM and Flowmove datasets for different cell sizes.

Fig. 7 shows the cell-by-cell comparison of vehicle kilometers for each cell size. For 100-by-100-m cells the Pearson correlation coefficient between vehicle kilometers per cell is 0.42. This is rather low because a) in ETDM many smaller roads are left out to reduce the computation time, b) ETDM uses population and road capacity as a proxy instead of traffic counts and modelling. Hence, concentrations around individual roads can differ from reality because of errors in the traffic intensities. But for larger cell sizes the Pearson correlation improves up to 0.96 for 10000-by-10000 m. This means that, despite the approximations, the ETDM traffic emissions are located not too far from where the really occur. This is important to estimate the traffic contribution at city level.

References

Amann, M., Borken-Kleefeld, J., Cofala, J., Heyes, C., Hoglund-Isaksson, L., Kiesewetter, G., Klimont, Z., Rafaj, P., Schöpp, W., Wagner, F., Winiwarter, W., Holland, M., Vandyck, T., 2020. Support to the Development of the Second Clean Air Outlook. Laxenburg.

Bächlin, W., Bösinger, R., Brandt, A., Schultz, T., 2008. Überprüfung des NO-NO2-Umwandlungsmodells für die Anwendung bei Immissionsprognosen für bodennahe Stickoxidfreisetzung. Reinhaltung der Luft 66, 154–157.

Berkowicz, R., 2000. OSPM - a parameterised street pollution model. Environ. Monit. Assess. 65, 323–331. https://doi.org/10.1023/A:1006448321977.

Bessagnet, B., Couvidat, F., Lemaire, V., 2019. A statistical physics approach to perform fast highly-resolved air quality simulations – a new step towards the meta-modelling of chemistry transport models. Environ. Model. Software 116, 100–109. https://doi.org/10.1016/j.envsoft.2019.02.017.

Carnevale, C., Finzi, G., Guariso, G., Pisoni, E., Volta, M., 2012. Surrogate models to compute optimal air quality planning policies at a regional scale. Environ. Model. Software 34, 44–50. https://doi.org/10.1016/j.envsoft.2011.04.007.

Degraeuwe, B., Pisoni, E., Christidis, P., Christodoulou, A., Thunis, P., 2021. SHERPA-city: a web application to assess the impact of traffic measures on NO2 pollution in cities. Environ. Model. Software 135. https://doi.org/10.1016/j.envsoft.2020.104904.

Degraeuwe, B., Pisoni, E., Thunis, P., 2020. Prioritising the sources of pollution in European cities: do air quality modelling applications provide consistent responses? Geosci. Model Dev. (GMD) 13, 5725–5736. https://doi.org/10.5194/gmd-13-5725-2020.

EEA, 2022. Air quality in Europe - 2022 report. Kopenhagen.

EEA, 2021. Air quality in Europe - 2021 report. Kopenhagen.

EEA, 2020. Air quality in Europe - 2020 report. Kopenhagen.

European Commission, 2022a. Proposal for a Directive of the European Parliament and of the Council on Ambient Air Quality and Cleaner Air for Europe. European Commission.

European Commission, 2022b. Annexes to the Proposal for a Directive of the European Parliament and of the Council on Ambient Air Quality and Cleaner Air for Europe (recast).

European Commission, 2022c. Proposal for a Regulation of the European Parliament and of the Council on Type-Approval of Motor Vehicles and Engines and of Systems, Components and Separate Technical Units Intended for Such Vehicles, with Respect to Their Emissions and Battery Durability (Euro 7) and Repealing Regulations (EC) No 715/2007 and (EC) No 595/2009. European Commission.

European Commission, 2022d. Proposal for a Directive of the European Parliament and of the Council Amending Directive 2010/75/EU of the European Parliament and of the Council of 24 November 2010 on Industrial Emissions (Integrated Pollution Prevention and Control) and Council Directive 1999/31/EC of 26 April 1999 on the Landfill of Waste.

FAIRMODE, 2022. Catalogue of measures [WWW Document]. URL. https://aqm.jrc.ec.europa.eu/measure-catalogue/. (Accessed 12 January 2022).

Hooyberghs, H., De Craemer, S., Lefebvre, W., Vranckx, S., Maiheu, B., Trimpeneers, E., Vanpoucke, C., Janssen, S., Meysman, F.J.R., Fierens, F., 2022. Validation and optimization of the ATMO-Street air quality model chain by means of a large-scale citizen-science dataset. Atmos. Environ. 272 https://doi.org/10.1016/j.atmosenv.2022.118946.

Isakov, V., Barzyk, T., Arunachalam, S., Naess, B., Seppanen, C., Monteiro, A., Sorte, S., 2017. Web-based air quality screening tool for near-port assessments: example of application in porto, Portugal, in: HARMO 2017 - 18th international conference on harmonisation within atmospheric dispersion modelling for regulatory purposes, proceedings. Hungar. Meteorol. Serv. 258–262. https://doi.org/10.1016/j.envsoft.2017.09.004.

Janssen, S., Dumont, G., Fierens, F., Mensink, C., 2008. Spatial interpolation of air pollution measurements using CORINE land cover data. Atmos. Environ. 42, 4884–4903. https://doi.org/10.1016/j.atmosenv.2008.02.043.

Jedlicka, K., Jezek, J., Kolovský, F., Kozhukh, D., Martolos, J., Stastný, J., Charvat, K., Hajek, P., Beran, D., 2015. OpenTransportMap [WWW Document]. URL. https://opentransportmap.info. (Accessed 28 November 2022).

Kiesewetter, G., Schoepp, W., Heyes, C., Amann, M., 2015. Modelling PM2.5 impact indicators in Europe: health effects and legal compliance. Environ. Model. Software 74, 201–211. https://doi.org/10.1016/j.envsoft.2015.02.022.

Kuenen, J., Dellaert, S., Visschedijk, A., Jalkanen, J.P., Super, I., Denier Van Der Gon, H., 2022. CAMS-REG-v4: a state-of-the-art high-resolution European emission inventory for air quality modelling. Earth Syst. Sci. Data 14, 491–515. https://doi.org/10.5194/essd-14-491-2022.

Lefebvre, W., Van Poppel, M., Maiheu, B., Janssen, S., Dons, E., 2013a. Evaluation of the RIO-IFDM-street canyon model chain. Atmos. Environ. 77, 325–337. https://doi.org/10.1016/j.atmosenv.2013.05.026.

Lefebvre, W., Van Poppel, M., Maiheu, B., Janssen, S., Dons, E., 2013b. Evaluation of the RIO-IFDM-street canyon model chain. Atmos. Environ. 77, 325–337. https://doi.org/10.1016/j.atmosenv.2013.05.026.

Maiheu, B., Lefebvre, W., Walton, H., Dajnak, D., Janssen, S., Williams, M., Blyth, L., Beevers, S., 2017. Improved Methodologies for NO2 Exposure Assessment in the EU (No. Report nr. 2017/RMA/R/1250). Study accomplished under the authority of the European Commission, DG-ENV Service Contract 070201/2015/SER/717473/C.3.

Mailler, S., Menut, L., Khvorostyanov, D., Valari, M., Couvidat, F., Siour, G., Turquety, S., Briant, R., Tuccella, P., Bessagnet, B., Colette, A., Létinois, L., Markakis, K., Meleux, F., 2017. CHIMERE-2017: from urban to hemispheric chemistry-transport modeling. Geosci. Model Dev. (GMD) 10, 2397–2423. https://doi.org/10.5194/gmd-10-2397-2017.

Ntziachristos, L., Samaras, Z., Kouridis, C., Samaras, C., Hassel, D., Mellios, G., McCrae, I., Hickman, J., Zierock, K.-H., Keller, M., Rexeis, M., Andre, M., Winther, M., Pastramas, N., Gorissen, N., Boulter, P., Katsis, P., Joumard, R., Rijkeboer, R., Geivanidis, S., Hausberger, S., 2020. 1.A.3.b.i-iv Road Transport 2022.

OpenStreetMap contributors, 2023. OpenStreetMap [WWW Document]. URL. www.openstreetmap.org. (Accessed 28 November 2022).

Pisoni, E., Clappier, A., Degraeuwe, B., Thunis, P., 2017. Adding spatial flexibility to source-receptor relationships for air quality modeling. Environ. Model. Software 90, 68–77. https://doi.org/10.1016/j.envsoft.2017.01.001.

Pisoni, E., Guerreiro, C., Namdeo, A., Gonzalez Ortiz, A., Thunis, P., Jannsen, S., Ketzel, M., Wackenier, L., Eisold, A., Volta, M., Nagl, C., Monteiro, A., Eneroth, K., Fameli, K.M., Real, E., Assimakopoulos, V., Pommier, M., Conlan, B., 2022. Best Practices for Local and Regional Air Quality Management. Joint Research Centre, European Commission. https://doi.org/10.2760/993882 version 1. Ispra.

Pisoni, E., Thunis, P., Clappier, A., 2019. Application of the SHERPA source-receptor relationships, based on the EMEP MSC-W model, for the assessment of air quality policy scenarios. Atmos. Environ. 4 https://doi.org/10.1016/j.aeaoa.2019.100047.

Rolstad Denby, B., Gauss, M., Wind, P., Mu, Q., Grøtting Wærsted, E., Fagerli, H., Valdebenito, A., Klein, H., 2020. Description of the uEMEP_v5 downscaling approach for the EMEP MSC-W chemistry transport model. Geosci. Model Dev. (GMD) 13, 6303–6323. https://doi.org/10.5194/gmd-13-6303-2020.

Simpson, D., Benedictow, A., Berge, H., Bergström, R., Emberson, L.D., Fagerli, H., Flechard, C.R., Hayman, G.D., Gauss, M., Jonson, J.E., Jenkin, M.E., Nyúri, A., Richter, C., Semeena, V.S., Tsyro, S., Tuovinen, J.P., Valdebenito, A., Wind, P., 2012. The EMEP MSC-W chemical transport model – technical description. Atmos. Chem. Phys. 12, 7825–7865. https://doi.org/10.5194/acp-12-7825-2012.

Thunis, P., Degraeuwe, B., Pisoni, E., Ferrari, F., Clappier, A., 2016. On the design and assessment of regional air quality plans: the SHERPA approach. J. Environ. Manag. 183, 952–958. https://doi.org/10.1016/j.jenvman.2016.09.049.

Thunis, P., Degraeuwe, B., Pisoni, E., Trombetti, M., Peduzzi, E., Belis, C.A., Wilson, J., Clappier, A., Vignati, E., 2018. PM2.5 source allocation in European cities: a SHERPA modelling study. Atmos. Environ. 187, 93–106. https://doi.org/10.1016/j.atmosenv.2018.05.062.

World Health Organization, 2021. WHO Global Air Quality Guidelines. Particulate Matter (PM2.5 and PM10), Ozone, Nitrogen Dioxide, Sulfur Dioxide and Carbon Monoxide.